Energy 282 (2023) 128401

Contents lists available at ScienceDirect

Energy

journal homepage: www.elsevier.com/locate/energy

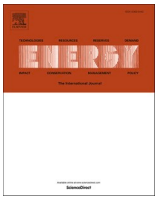

Design optimization of compact gas turbine and steam combined cycles for combined heat and power production in a FPSO system–A case study

Rubén M. Montañés [a,*], Brede Hagen [a], Han Deng [a], Geir Skaugen [a], Nicolas Morin [b], Marius Andersen [b], Marit J. Mazzetti [a]

[a] SINTEF Energy Research, Gas Technology, NO-7465, Trondheim, Norway
[b] SINTEF Industry, Materials and Nanotechnology, NO-7465, Trondheim, Norway

ARTICLE INFO

Handling Editor: L Luo

Keywords:
Process optimization
Energy efficiency
Mechanical integrity
Vibrations
Thermal stresses
Water treatment

ABSTRACT

This case study aims to cover a wide range of relevant aspects related to combined cycle design, mechanical integrity and operational reliability for cogeneration of heat and power in FPSO systems. The methods consist of combined optimization of combined cycle thermodynamic design and geometry of steam generator; vibration analysis for flow induced vibrations; and thermal stress estimation of casings during cold start-stop scenarios. Challenges and opportunities for reliable water treatment systems are explored. The results show that small tubes, a compact tube bundle and a low condensation temperature reduces the once-trough steam generator (OTSG) weight. The vibrations numerical simulations in this work support the standard recommendations of using 35 times tube OD as upper limit for the unsupported tube length, which could be used as a reasonable design criterion. Thermal stresses analysis indicates that the design of beam arrangement, location, and stiffness of beams has a major impact on thermal stresses, and can be optimized to different plate thicknesses in order to avoid fatigue damage. Focus should be on reducing leaks of deaerator, steam turbine and condenser. It is recommended to add Na sensors after condenser and investigating the use of Electrodeionization (EDI) technology for make-up water production from seawater.

1. Introduction

Offshore oil and gas production is a very energy intensive process and the gas turbines used for power generation on offshore energy systems generate 85% of the emissions on the Norwegian Continental Shelf (NCS) [1]. These turbines are therefore the main target for offshore emission reductions [2]. The exhaust from these turbines has a relatively high temperature (ca. 400–600 °C) and contains more thermal energy than the heat demand on offshore facilities. Thus, converting the excess exhaust heat to power will increase fuel efficiency and therefore reduce CO_2 emissions. This can be achieved by adding bottoming cycles. Indeed the installation of bottoming cycles can result in a reduction of CO_2 emission of approximately 25% per retrofitted platform [1]. There are three bottoming cycles installed on the Norwegian Continental Shelf. Based on operational experience from these systems there are several areas where there is potential for improving the combined cycle technology so that it is better suited for offshore installation and can become standard technology for offshore power generation rather than the exception it is today [1–3].

In the offshore oil and gas industry, an alternative system to offshore platforms, the FPSO (Floating Production, Storage and Offloading) platforms, can lead to advantages. This includes the possibility to operate petroleum maritime fields located in remote areas [4,5]. A FPSO is a floating facility needed to perform operations of production of petroleum. FPSOs could incorporate a combined cycle to increase efficiency and reduce emissions [4].

The reduction of CO_2 emissions from oil and gas production on FPSOs has been addressed in previous work by Barbosa et al. [4]. That work aims to evaluate different cogeneration plants usually used in FPSOs, using cold deep sea water to improve efficiency of the cogeneration plants. This cooling subsystem uses sea cold water to cool inlet air of gas turbines (GT) and reciprocating engines as well as the steam plant condenser. The off-design operation for the main equipment is taken into account since electrical and thermal demands present significant variations along life of the oil field. The results showed that the additional cooling subsystem using deep sea water increased the exergy

* Corresponding author. Department of Gas Technology, SINTEF Energy Research, Sem Saelands vei 11, 7034, Trondheim, Norway.
E-mail address: ruben.mocholi.montanes@sintef.no (R. M. Montañés).

https://doi.org/10.1016/j.energy.2023.128401
Received 30 March 2023; Received in revised form 12 June 2023; Accepted 10 July 2023
Available online 20 July 2023

efficiency 2.5% for gas turbines giving a reduction of 128,585 t of CO_2 emissions. For a steam plant the increase in exergy efficiency was 2.9% [4]. In a paper by Silva and Oliveira [6] the exergy cost for oil and gas produced on a Floating Production Storage and Offload (FPSO) ship is evaluated along the lifespan of the well taking off-design operation conditions of process plant and cogeneration plant into account. The impact of three different cogeneration plants and two different process plant operating modes was assessed. The reciprocating engine proved to be the most efficient technology (lowest unit exergy costs and CO_2 emissions), although reliability, weight, size and monetary costs have to be evaluated. The work show that significant reductions of fuel consumption and CO_2 emission can be achieved by integrated process optimization approaches [7].

Combined cycles onshore have reached high lower heat value (LHV) efficiency - normally by using three-pressure-reheat systems - and standardization [8], and high levels of operational flexibility [9,10], combined with potential for large decarbonization [11]. On the contrary, combined cycles offshore are more challenging to standardize. Several challenges have prevented the widespread implementation of combined cycles in offshore energy systems, that are mostly driven by gas turbine systems for power production in brownfield applications [12,13]. In previous units installed offshore there has been evidence of cracking of the outer tubes in the heat recovery steam generator (HRSG) due to vibrational damage and fretting. Also the casing of the waste heat recovery unit has been subject to failures. In this case study, the focus is therefore on understanding better factors that cause decrease in operational reliability and investigate potential design improvements, at conceptual design stage.

A combined process and heat exchanger geometry optimization approach allow to explore designs with low weight-to-power ratio, as shown for power-only combined cycles [14,15]. The equipment contributing the most to total weight is the heat recovery steam generator (HRSG). And therefore, options for bringing weight down have been reported in the literature. Once through steam generators (OTSG) are the common choice when striving for low weight and volume footprint [16]. A potential for weight reduction of the steam cycle of over 50% was reported by Mazzetti et al. [2], the reduction in footprint was also over 50%. A key parameter in achieving weight reduction is in reducing the diameter of the tubes of the OTSG [2]. A reduction in tube diameter gives increased weight reduction of the unit [14]. Techno-economic optimization has been proposed, however it is highly uncertain in offshore [17], specially at conceptual design phase.

In the size optimization process, focus has been on the heat recovery steam generator, which is the main contributor to the mass of the offshore bottoming cycle [2]. To reduce the weight of the system, different configurations of pipe dimensions, materials, and bending radii have to be investigated. Structural limits of the pipes that undergo the necessary bending operations have to be established, in order to determine the feasibility of the operations. The pipes used in waste heat recovery units are cold bended by using rotary-draw bending machines. In the process, a tube to be bent is clamped with a die, rotated around another die, and at the same time push at its end, in order to obtain a bend with the best cross section, and lowest wall thinning on the outer part of the tube. Structural problems arise during bending of tubes, either geometrical or material based. The main quality aspects in tube bending are validation of cross-section, excessive thinning of tube wall, wrinkling of the side on the inner side of the bend, or fracture due to excessive strains. Bending limits have been established against different issues in the literature, as in Zhao et al. [18] or Khodayari [19]. Some authors have taken it further, looking at differential heating of the bend to break the forming limits as in Ref. [20] or [21]. The need in the heat exchanger optimization algorithm was to establish a minimum bending radius that was manufacturable for the partners, using cold rotary-draw bending for some chosen materials.

Given the required capital investment of the equipment in a bottoming cycle, the fact that the bottoming cycle might be production critical, and the engineering challenges of maintenance and expensive manning offshore, robust bottoming cycle design is crucial. However, the bottoming system must also be reliable, and should cover flexible demands across multiple scales, normally called cyclic operation. Robust control structures for transient load changes [22–24] and start-up [16] are required. Cyclic operation might result in early equipment failure due to several mechanisms, including creep-fatigue phenomena in thick-walled components [25]. Therefore, further research on mechanical integrity and modelling of thermal stresses in bottoming cycles offshore is required. The principal mechanisms of failure of high temperature components in power plants include flow-induced vibrations of tube bundles [26]; and creep, fatigue, creep-fatigue and thermal fatigue [25,27] of thick-walled components. Knowledge on mechanical integrity issues in the literature is mostly reported for onshore combined cycle applications, due to the widespread implementation, operational hours of the technology, and recent research conducted on thermal stresses. However, knowledge on the principal mechanisms of failure is scarce for offshore applications.

As for the heat exchanger to fulfil its purpose, the gas flow needs to be conducted across the tube bundle in a defined volume. The tube bundle needs to be hold in place, by a frame, while a casing directs the exhaust gas flow optimally through the tube bundle. There are mainly two types of casing, hot and cold. In hot casing, the casing is in direct contact with the exhaust, and must withstand its extreme temperature, as well as the temperature gradient at start and stop of the gas turbine. In cold casing, an additional function of the casing is to hold in place an insulation layer by the means of an internal liner. The temperature of the casing stays low, below 60 °C degrees, which is sometimes the requirement (ISO 21905:2020). Start and stop cycles of the gas turbine result in alternative expansion and contraction of the different parts of the casing. Thin parts closest to the exhaust flow warm up faster than thicker flanges and stiffeners, further away from the flow. Those differences cause low cycle fatigue of the casing, that may cause problems before the design lifetime of the structure. Numerical methods are used to simulate the operation of the turbines, and predict the lifetime of the design [28,29].

Flow-induced vibrations can be a critical issue to be considered for the HRSG, particularly for the lightweight designs. Many real-life cases in the power-generating industry where flow-induced vibrations occur result in serious damages; refer to the work described by Paidoussis [26]. Most of the studies from literature focus on the vibrations of the heat exchangers with conventional tubes normally having large diameter and no fins, while there only exists a few studies for vibrations of lightweight finned tube bundles, like Deng et al. [3] for design optimization, and Zhang et al. for experimental [30] and numerical assessments [31,32] of flow induced variations in tube bundles.

Condensate purification is key to the steam cycle operation. Also, for the water purification system the main goal has been to reduce weight to allow broader implementation of the steam cycles on existing brownfield plants as well as greenfield. Previously published systems have had high leak rates and therefore needed large amounts of make-up water which meant large water treatment systems and holding tanks. The first step was therefore to reduce leaks. The water treatment is also quite labour intensive as the ion exchange bed filters require close follow up of water quality and regeneration quite frequently. This work investigated means to make the water treatment process more automated and operationally reliable. One potential improvement is the use of Electrodeionization (EDI) technology. EDI is a relatively light weight technology which is important for brownfield implementation. In earlier work electrodeionization has been shown to have good operational reliability [33]. Another focus has been to further increase operational reliability of the system by adding new sensors to improve monitoring and therefore ensuring consistent water quality.

The requirements and specifications for combined cycle and steam bottoming cycle designs in offshore installations are highly dependent on the site, and therefore must be addressed via case studies. The

majority of case studies of compact bottoming cycles offshore are based on offshore platform specifications. In this work, a case study of an FPSO system is defined. It must provide heat and power. The aim is to cover a wide range of relevant key aspects related to combined cycle design, in brownfield applications. A key factor for widespread implementation is reduced weight and footprint. Another key combination of factors is mechanical integrity and operational reliability. For the FPSO system, bottoming steam cycle design optimizations are carried out, with focus on thermodynamic optimizations of the steam cycle to meet the demands while optimizing the heat exchanger design to minimize OTSGs weight, based on the methodology by Mazzetti et al. [2] and Hagen [34]. The design for different tube selection and condensation temperature is evaluated with respect to weight considerations of the OTSG and thermodynamic cycle design optimization. A novelty of the present work is the constraint used to limit the diagonal tube pitch. Flow-induced vibrations for the OTSG designs are examined by the methods presented in Deng et al. [3], and required number of plates is discussed. A casing design is selected for further evaluation of thermal stresses for start-stop scenarios in gas turbine operation, under which the equivalent plastic deformations that lead to damage, compared for different beam arrangements and plate thicknesses of the casing. Finally key aspects of water treatment and innovative systems are discussed.

2. Methodology

2.1. Case study definition: combined cycle combined heat and power plant in a FPSO

The reference FPSO case is a power generation system consisting of three gas turbines. Three gas turbines are implemented in simple cycle for power production, providing 86 MW_{el}. On offshore installations, the gas turbines commonly operate in load sharing mode, meaning that two or more engines divide the load equally. In the reference case, the gas turbines all sharing the same load, at ca. 71.67% load. To remove one gas turbine from continuous operation and hence increase efficiency and reduce CO_2 emissions, the case study explores installing a steam bottoming cycle. Fig. 1(a)) shows the combined cycle combined heat and power (CHP) configuration system.

For the combined cycle, the standard configuration is utilized, in which the exhaust gas from two SGT-750 turbines is utilized to provide heat in two heat recovery steam generators, with steam produced to meet the heat and power demand of the surrounding energy system. In order to achieve a low weight and a compact system, the HRSG selected is of the once-through steam generation (OTSG) type. The CHP power plant provides a power demand of overall 86 MW_{el} and 10 MW_{th} heat. Table 1 summarizes the case study definition. In addition, Fig. 1(b)) shows the bottoming cycle flowsheet model.

The CHP combined cycle power plant configuration consists of.

- Two gas turbines Siemens SGT-750 [35]. At bottoming cycle design point, the gas turbines are operated in load sharing mode and provide 72 MW_{el}. This is, 36 MW_{el} each GT, being equivalent to 90% load.
- Two OTSG systems recover heat from the exhaust of the gas turbines to provide steam.
- Steam turbine with a high-pressure (HP) section and a low-pressure (LP) section.
- Steam turbine with steam extraction for heat production. A heat demand of 10 MW_{th} should be provided by the system. The heat carrier fluid is heated up from 40 °C to 120 °C in the heater condenser.

2.2. Bottoming cycle design optimization

The bottoming cycle design optimizations were carried out using a mathematical models of the bottoming cycle integrated with a gradient-based optimization algorithm NLPQL [36]. The mathematical model governs a thermodynamic model of the bottoming cycle process and a more detailed model of the OTSG. The thermodynamic model considers the thermodynamic state points at the inlet and outlet of each component. The water/steam state points are defined by pressure and specific enthalpy. Once these two properties are defined the remaining thermophysical properties were computed using the implementation of the IAPWS formulation including its equations of state (EOS) from Ref. [37]. The exhaust gas state points (OTSG inlet and outlet) are defined by

Table 1
Comparison of the proposed combined cycle system for generating 86 MW_{el} and 10 MW_{th} with a Gas turbines only solution.

	Gas turbines only	Proposed combined cycle
Gas turbine model	SGT-750	SGT-750
Number gas turbines	3	2
Gas turbine load	72%	90%
Gas turbine CO_2 emissions	19.3 kg/s	15.3 kg/s
Gas turbine power production	86 MW	72 MW_{el}
Bottoming cycle power production	0 MW	14 MW_{el}
Total power production	86 MW	86 MW_{el}
Total heat production		10MW_{th}

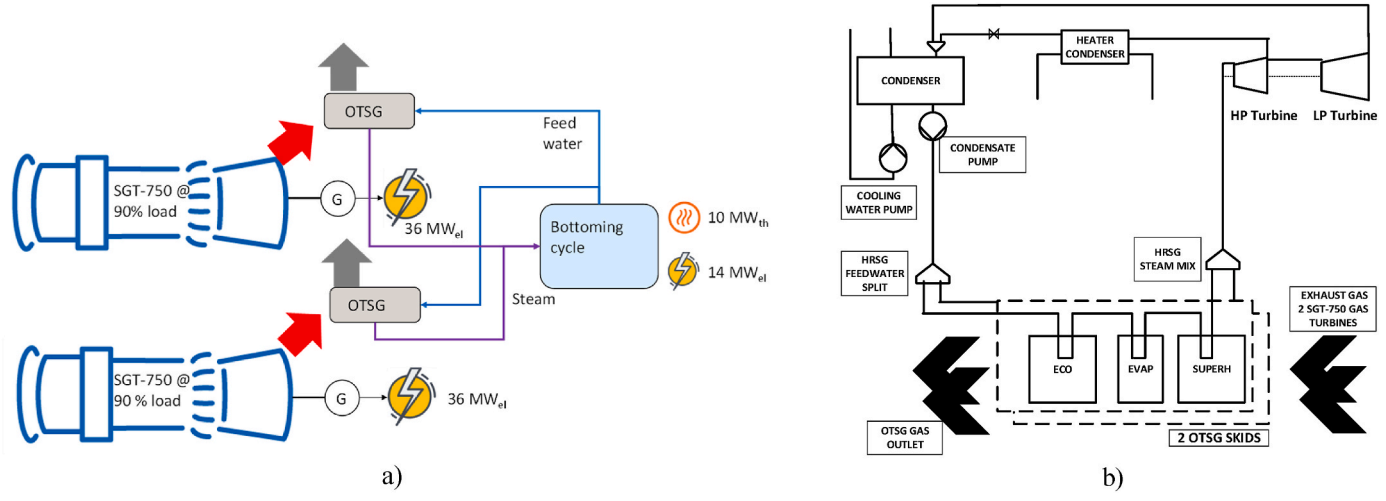

Fig. 1. a) Combined cycle configuration with two SGT750 gas turbines, two OTSGs and the bottoming cycle and process boundary conditions for FPSO case. b) Bottoming cycle flowsheet model.

pressure and temperature. The remaining properties in these state points were computed using the implementation of the EOS. The heat fluid that delivers 10 MW_{th} thermal energy between 80 °C and 120 °C and is assumed to have a heat capacity estimated with the IAPWS formulation. Furthermore, the location of the minimum temperature difference, commonly referred to as the pinch point, of the heat condenser is located at the point where steam condensation starts, see Fig. 11. This means that the heat condenser pinch point temperature difference (PPTD) can be computed exactly. The thermodynamic model uses prescribed values for isentropic efficiencies to compute the outlet enthalpy of the pump and the turbines. The net power output is computed as the difference between the electric power generated by the steam turbines and the power consumed by the feedwater pump, accounting for electromechanical conversion.

The OTSG model uses the thermodynamic state points at the hot end and OTSG core geometry information, see Table 2, to compute the fluid pressure drop and OTSG size and weight. The OTSG model use semi-empirical correlations for estimating local heat transfer and pressure drop. Furthermore, the OTSG model takes the advantage of an efficient solution procedure that enables solving the OTSG by means of a once-through calculation. This procedure starts at the lowermost tube row (hot end) and continues tube row by tube row until the predefined OTSG duty, defined by the exhaust gas outlet temperature, is reached. The reader is referred to Mazzetti et al. [2] and Hagen [34] for further information on the semi-empirical correlations within the OTSG model and the novel solution procedure, respectively. Skaugen et al. [38] developed a methodology for optimizing total minimum weight of an off-shore waste heat recovery unit by including both the finned tube bundle and the casing and structures. The result showed a close to quadratic exhaust gas flow area to keep the total weight low. The casing and structures are also accounted for in this work, following the model formulation in Ref. [38]. Duct plate thickness of 8 mm is chosen in this work.

The mathematical formulation (fixed parameters, independent variables, constraints, and objective function) of the bottoming cycle design optimization method is summarized in Table 2

Table 2
Mathematical formulation of the bottoming cycle design optimization.

Fixed parameters	Exhaust gas temperature	443.3 °C
	Exhaust gas mass flow rate	112.5 kg/s[a]
	Turbine isentropic efficiency	0.85
	Pump isentropic efficiency	0.70
	Electromechanical conversion efficiency	0.95
	Condensation temperature	30°C and 40°C
	OTSG tubes	¾" and 1 ¼", see Table 3
	OTSG tube material	Inconel 825
	OTSG fin thickness	1.05 mm
	OTSG tube layout angle	30°
Independent variables	Intermediate pressure level	
	Pump outlet pressure	
	Turbine inlet pressure	
	Turbine inlet enthalpy	
	Exhaust gas outlet temperature	
	OTSG tube length	
	OTSG number of tubes per row	
	OTSG fin tip clearance	
	OTSG fin pitch	
	OTSG fin height	
Constraints	Consistent pressure at pump outlet	
	Net power output	14 MW
	LP turbine outlet quality	> 95%
	Exhaust gas pressure drop	< 30 mbar
	PPTD in the heat condenser	> 10 K
	Minimum diagonal tube pitch	See Figure 3
Objective function	Minimize OTSG total weight	

[a] From each gas turbine and within each OTSG.

Table 3
OTSG tubes considered in this work.

Tube identifier	¾"	1 ¼"
Outer diameter (OD)	19.05 mm	31.75 mm
Wall thickness (t)	1.65 mm	2.11 mm

The fixed parameters are selected and do not change during the optimization. Notably the fixed parameters govern the OTSG tube geometry. This work considers two different OTSG tubes whose geometry are shown in Table 3. In the remaining part of this paper, these tubes are referred to by the identifier that express the tube outer diameter in inches.

All independent variables indicated in Table 2 were manipulated by the optimization algorithm with the aim of minimizing the objective function and satisfy the constraints. The independent variables of this work include both thermodynamic parameters of the bottoming cycle process and OTSG core geometry parameters. Each independent variable was constrained between a lower and an upper bound. The numerical values for these bounds were selected such that the optimal solution was not excluded by any bounds.

The optimization algorithm facilitates the use of both equality and inequality constraints. They can be imposed to ensure a consistent and a feasible design. An equality constraint was imposed to ensure that the water inlet pressure computed by the HRSG model were equal to the pump outlet pressure defined as an independent variable. An equality constraint was also imposed to ensure that the bottoming cycle delivers the desired net power output. A novelty of the present work is the constraint used to limit the diagonal tube pitch. In our previous work we constrained the diagonal tube pitch be larger than 3 times the outer tube diameter [2]. This boundary was set based on personal communication with an HRSG manufacturer claiming that the bend diameter should be larger than 3 times the outer tube diameter. In this work we made an attempt of challenging this *guideline*.

Compactness of the heat exchanger is directly linked to size of the tube bundle. Reduction in the size of the tube bundle will result in reduction of overall heat exchanger size. Key to achieve this is to manage to produce tubes with bends tighter than the actual industry bending limit of 3 times the outer tube diameter. As to study the structural limits of rotary-draw bending operations, numerical investigations have been performed on the bending process of tubes of different dimensions and materials to determine limits of the manufacturability.

Main problems that arise during rotary-draw bending operations are ovalisation, thinning, wrinkling and collapse of the cross-section (see Fig. 2).

Finite element models were established for cold rotary-draw bending of 3 different steels, AISI 304 [39], SUS 304 L [40] and Inconel 825 [41]. The constitutive material models (Hollomon for the first 2, Voce for the latter) used for the analyses were taken from the literature.

A test matrix combining materials, wall thickness, bending factor was established to determine combination of factors (see Table 4). Acceptance criteria have been set for the study for the three quality parameters, ovalisation, wrinkling and thinning. For further work with the investigations, criteria can be found in EN 12952. In this case study, the criteria were set as follow: for ovalisation, the criterion is set to 20% of change; for wrinkling, the criterion is set to a twist of 0,05 rad/mm and the criterion is set to 10% thinning.

The outcome from the bending analysis is summarized in Fig. 3. Simulation results were post-processed to be assessed against each aforementioned criterion. The check against each criterion were then put together to a single OK/NOT OK assessment, where each single negative value resulted in not acceptable bend quality, NOT OK. Thicker tubes (with the smallest wall thickness factor) passed the bending analysis for bend diameters as low as 2.3. The figure also suggests that the minimum bend diameter for the OTSG tubes of this work is significantly lower than the previous lower limit of 3.0 and is not constant but

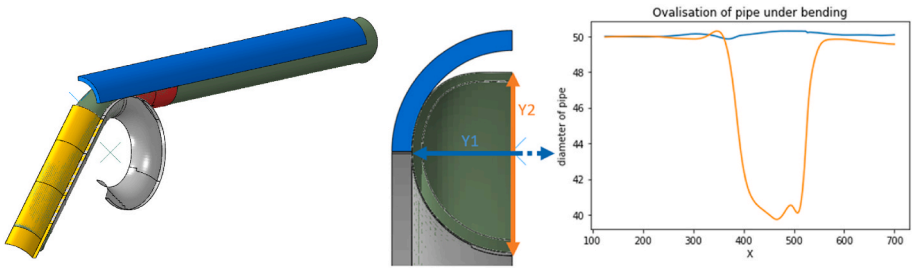

Fig. 2. Rotary-draw bending operation, half model in FEA (left) and example of problem (ovalisation of the cross section (right).

Table 4
Parameters for the determination of the test matrix (WF, wall thickness factor, BF, Bending factor, OR, outer tube diameter).

Parameter evaluated	Values
WF	10, 12, 15, 20, 25, 30
BF	1, 1.15, 1.3, 1.5
OR	25
Material	SUS304L, AISI304, Inconel825

depends on the wall thickness factor.

The objective of the optimization is to minimize the OTSG weight. This weight includes the core whose weight is computed using geometric description of the tube and fins and the material density. We also made an attempt of estimating weight of the tube bundle support plates, beams and duct plates. Thus, the objective function refers to the to the total weight of the OTSG. The reader is referred our previous publications [2,34] for further information on framework and structure model.

2.3. Flow-induced vibrations

The flow-induced vibrations for the OTSG designs were examined by the methods presented in Deng et al. [3]. The four main vibration mechanisms, turbulent buffeting, vortex shedding, fluid elastic instability, and acoustic resonance, were considered for the finned tube bundles in the crossflow configuration.

Each tube row of the finned tube bundle is divided into end and middle tube spans by the support plates. For the OTSG designs, two support plates are used as default, which gives two end tube spans and one middle tube span. The length of each span is equal. For the turbulent buffeting, the root mean square of tube deflection y_{rms} is calculated for the end and middle span of each tube from an empirical correlation, and it should be smaller than 2% of the tube outer diameter to ensure the design robustness. The vortex shedding and acoustic resonance are excited by the coincidence of the frequencies. The vortex shedding frequency f_{vs} and the acoustic resonance frequency of mode 1 and mode 2 $f_{a,j}(j = 1, 2)$ are calculated. The corresponding lock-in conditions are needed to be avoided, namely $0.8 < f_{vs}/f_n < 1.2$ for vortex shedding, and $0.8 < f_{a,j}/f_{vs} < 1.35$ for acoustic resonance. For the fluid elastic instability, the critical flow velocity U_{crit} is calculated and the maximum flow velocity U_{max} should be smaller than $0.8U_{crit}$.

The OTSG designs were evaluated for the four vibration mechanisms. Then it is checked if the designs satisfy the design criteria. If the criteria cannot be met, one possible solution is to reduce the length of the tube span by adding more support plates until the vibrations are within the safe range. In general, a shorter tube span will give a larger stiffness [3]. Fig. 4 shows the original design uses 2 middle support plates with 3/4″ tube. The main purpose of checking the vibration 'off-line' is for obtaining a robust design, rather than letting the vibration constraints affect the design too much, given that other design constraints have higher priority.

2.4. Thermal stresses

Under heating of the casing, thermal expansion gives rise to stresses where plates and stiffeners are restrained from displacement. The casing design, location of stiffening beams play an important role in the distribution of the stresses on the casing.

Start and stop of the gas turbine leads to a heat flux on the inside of the casing, gradually heating up the inner surface. Heat transfers to structural part by conduction from inner to the outer surface; stiffeners on the outside of the casing will reach high temperature later than the casing plates. Differential heat expansion resulting from uneven temperature will cause deformations of the casing structure. Where the deformations overcome the elastic limit of the material, plastic deformations occur, and damage is developing. If it happens at each

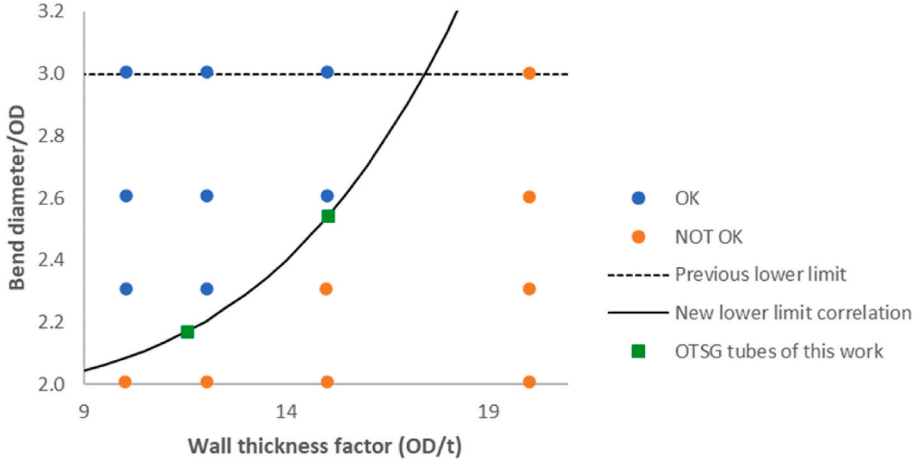

Fig. 3. Graphical illustration of the outcome from the bending analyses of Inconel825 tubes and the new lower limit for the bend diameter and thus the diagonal tube pitch.

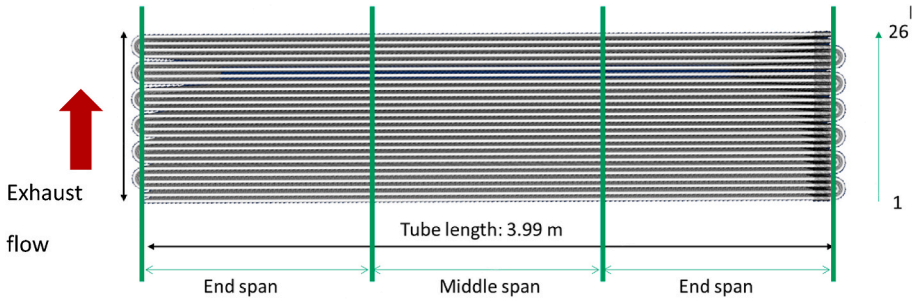

Fig. 4. Original OTSG bundle configuration design with tube plates in green. The evaluation of flow-induced vibrations based on the HRSG geometry consider vibrations from the 4 main mechanisms. If vibrations exceed the limit, we add more support plates to reduce the length of tube span.

heating-cooling cycle, damage increases and will lead to low-cycle fatigue, that could case failure after only limited number of cycles.

A numerical model has been set up to investigate the behaviour of the casing during heat up and cool down transients. Cold start-ups are key transient elements leading to large thermal stresses [16]. The purpose of the model was to evaluate the effect of plate thickness on the casing's ability to withstand thermal stresses. The aim for the case study is to minimize the mass of the OTSG, of which the casing represents an important part.

The case for small tube diameter (3/4″ in tubes, 1.5OD), found as an optimum by the algorithm was chosen as a case, and is used for the geometry of the OTSG.

The casing is modelled with Finite Elements (FE). The model is made of a fourth of the casing (see Fig. 6), with plates structures, meshed with shell elements (see Fig. 5). Stiffeners defined by the algorithm are also modelled by shell elements, to be able to account for contribution to rigidity and heat capacity.

The casing taken as an example is an idealization of the OTSG and casing, which finds an optimal mass and compactness for the heat exchanger. It does not represent an industrial design casing, and thus limits the conclusions that can be drawn from the numerical investigations. The purpose of them is solely to see trends and pinpoint design recommendations for casing design. Design of such a structure is a complex task, and determination of plate thickness, stiffeners arrangements, flange design, expansion joint design are iterative tasks. However, some general findings can facilitate the design of such a structure.

The chosen casing geometry was studied against a heat flux of 5 kW/m^2, that was applied homogeneously on the whole inside surface of the casing. This is an ideal model to represent a hot casing, or a cold casing

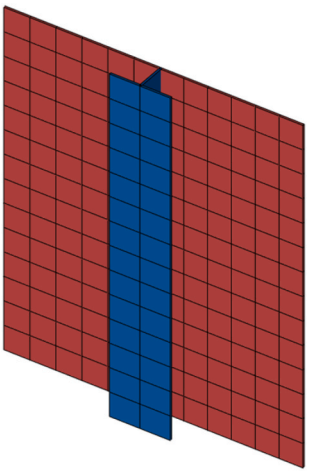

Fig. 5. Example of casing plate and stiffener meshed with shell elements.

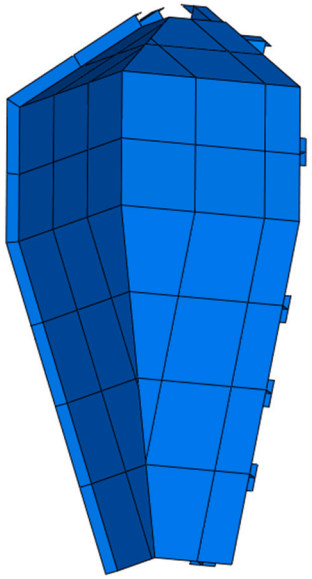

Fig. 6. CAD model of a fourth of the casing.

where insulation has failed. Such a choice was made in order to see the effect of high thermal deformations on the behaviour and stress and strain development on the casing. The heat flux chosen was determined as to achieve a plausible heat-up time for the casing, based on a measure made by an operator on one of their exhaust systems. Cooling with a negative heat flux of the same value was used for this case, which is a plausible assumption based on discussions with the operator, when blowing cold air through the casing. Two start-stop cycled were simulated, corresponding to heat from 20 °C to 500 °C, followed by cooldown to 20 °C, twice, see Fig. 7. The duration of the cycles was determined as to achieve the max temperature with the chosen heat flux, and revert it to reach start temperature, and repeating it two times. Temperature distribution can be seen on Fig. 8. The results that were studied were the

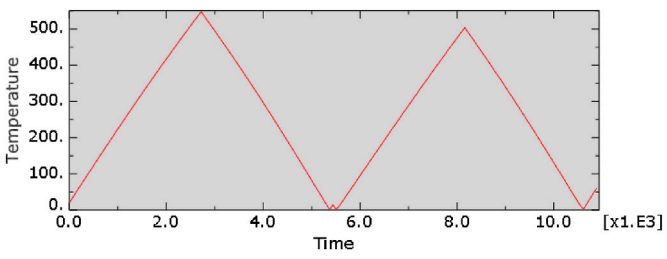

Fig. 7. Temperature [° C] cycles caused by the heat flux as a function of time [s].

equivalent plastic deformations that lead to damage, compared for different beam arrangements and plate thicknesses of the casing, see section about results.

2.5. Water purification system design

The water treatment system consists of fluid holding tanks which make up 60% of its total weight. This is partially due to a high leak rate in previous steam turbine combined cycle systems requiring a high rate of makeup water production and purification of about 20 tonnes per day. The potentially biggest reduction in the water treatment system weight would therefore come from reducing the number of leaks. An analysis was performed for the different components of the water treatment system to identify sources of leaks and means to reduce these.

Beyond that, changes must be made to the previously published systems which in some cases struggled to meet the required purity of condensate. The conductivity of the water should be at 0.2 μS/cm for a steam cycle according to IAWPS [37]. Water analysis data has shown that it has been up to the 1–2 μS/cm range during operation in some cases. Better operational and monitoring routines must therefore be developed for the water treatment systems. It is believed that EDI could give a stable high quality of deionized water as it will run continuously without the need for manual regeneration. A water treatment system based on use of EDI was therefore designed and dimensioned.

3. Results and discussion

3.1. Design optimization results

Four bottoming cycle design optimizations were carried out considering two different OTSG tubes and two different condensation temperatures in the steam turbine condenser. The minimized OTSG weight from these optimizations are shown in Fig. 9. The results are summarized in Table 5.

The results in Fig. 9 confirm that the tube selection is a key driver for low weight. Small tubes lead to lighter OTSGs. For the cases with 30 °C condensation temperature, ¾" tubes leads to ca. 32% total weight reduction in comparison with the OTSG design based on 1 ¼" tubes. The core (tube bundles) represents 37–41% of the total OTSG weight, while the frame represents 42–45% of the total weight. In Fig. 9 it is also low condensation temperature yields lower OTSG weight (ca. 3 tons lower) but it has less impact than the tube diameter. However, it could also lead to a larger condenser and LP steam turbine (larger volumetric flow at lower condensation temperature).

Fig. 10 shows the total weight of a single OTSG for designs using previous bend limit (diagonal tube pitch three times the tube diameter 3 *x* OD) compared to the results with new bend diameter suggested in this work. The results shown in Fig. 10 include eight optimization cases considering 30 °C and 40 °C condensation temperature, for OTSG designs based on ¾'' and 1 ¼" tubes. The results in Table 5 show that a smaller diagonal tube pitch is obtained than previously. The optimization selected the lower bound for the 1¼" OTSG tube cases. A relatively low turbine inlet pressure is obtained. It cannot be higher due to the LP turbine outlet vapor quality constraint (not shown). Results in Fig. 10 and Table 5 indicate that using smaller bend diameter than current design practice, can lead to OTSG designs of lower weight.

The optimized process is visualized in Fig. 11 that shows T-s diagrams of the optimized bottoming cycle processes using the ¾" OTSG tubes. Two cases are shown for condensation temperature: 30 °C Fig. 5 (a) and 40 °C Fig. 5(b). The corresponding T-s diagram obtained for the 1 1/4" tubes are very similar, not shown. Most notable difference between the two T-s diagrams is the condensation temperature. The condensation temperature might have implications with respect to water treatment system selection so must be considered in conjunction with performance of water treatment system.

3.2. Flow-induced vibration analysis results

Figs. 12 and 13 shows the vibration analysis for the two designs of ¾" OTSG tubes and 1¼" OTSG tubes for the 30 °C condensation temperature. As mentioned before, two support plates were used as default design. As we can see from Fig. 12(a), (b), (d), the original design with ¾" OTSG tubes and two plates is sufficient to limit the vibration within the safe range. However, the maximum flow velocity at the middle tube span of the first tube row is about 1.8 times of the critical flow velocity, as shown in Fig. 12(c). This could result in severe fluidelastic instabilities. Two more support plates are needed to increase the critical velocity and thus reduce the ratio of U_{max}/U_{crit}. For the design with 1¼" OTSG tubes and two plates, one more support plate is required to satisfy the criterion to mitigate the fluid-elastic vibration, as shown in Fig. 13 (b). The vortex shedding and acoustic resonance for this design is in the safe range and the plots are omitted here.

With adding more support plates, the tube span length for the design with ¾" OTSG tubes is reduced to about 0.8 m, and 1.3 m for the design with 1¼" OTSG tubes. This is slightly higher but close to the design standard (ISO13705:2012) of using 35 times of the tube OD as the upper limit for the unsupported tube length, corresponding to 0.67 m and 1.11 m for ¾" and 1¼" tubes. Adding support plates also adds weight. The increased weight from the support plates is 590 kg (design with ¾" OTSG tubes) and 852 kg (design with 1¼" OTSG tubes).

3.3. Thermal stress

The numerical study leads to observation of higher plastic strains at the vicinity of beam connections with higher thickness, where beam stiffeners are stiffly connected to each other, while other places on the structure, plastic strains are lower after 2 cycles for the thinner plate thickness. Fig. 14 shows the detail view for 3 different plate thickness (6, 8 and 12 mm from left, top) showing equivalent plastic strains after 2 cycles.

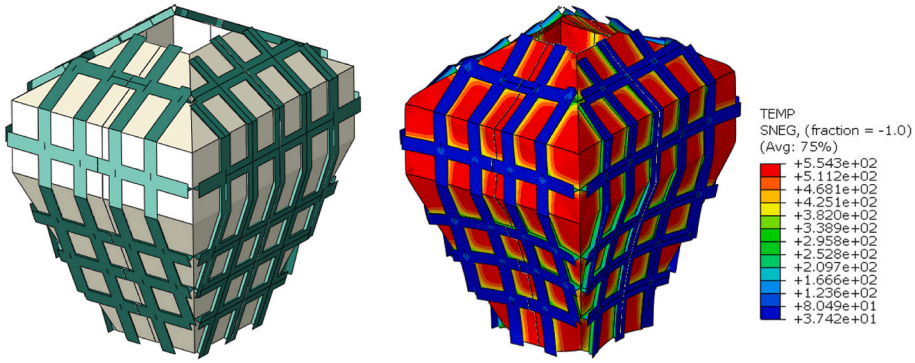

Fig. 8. Full model of casing (mirrored for visualization) that reached exhaust temperature [ºC].

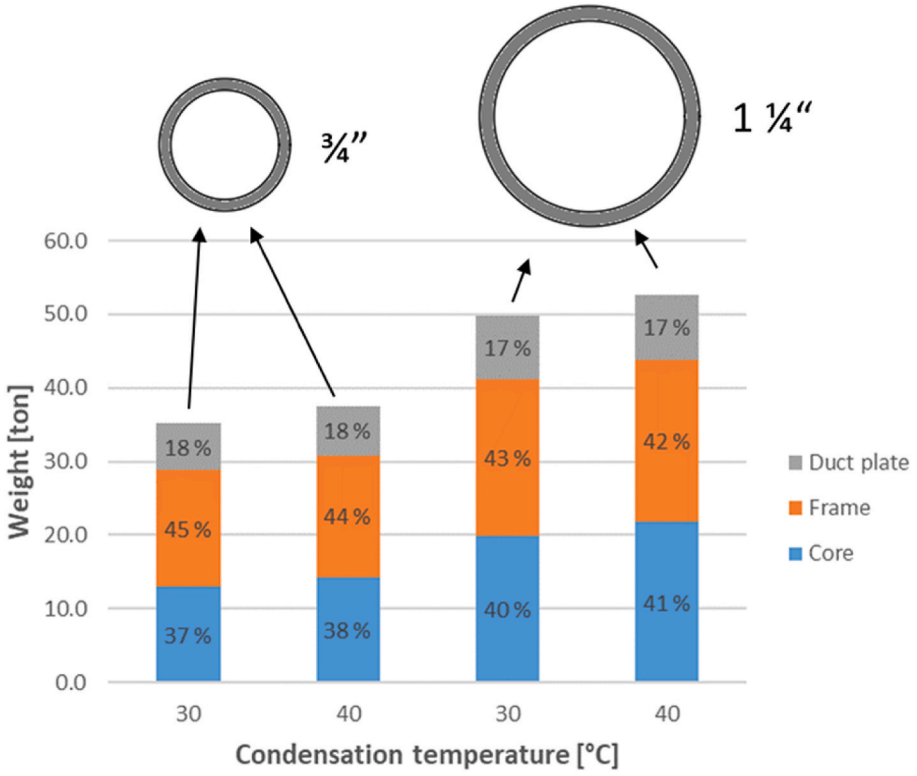

Fig. 9. Minimized OTSG weight from bottoming cycle design optimization considering two different OTSG tubes (visualized at the top) and condensation temperatures. The heat and power production are identical in all cases. The results are for the new bend diameter in this work.

Table 5
Selected numerical values of process parameters and OTSG core geometry of the optimized bottoming cycles. All cases have the same heat and power production.

Case	OTSG tube Bend constraint	¾”	¾” 3xOD	¾”	¾” 3xOD	1 ¼”	1 ¼” 3xOD	1 ¼”	1 ¼” 3xOD
definition	Condensation T [°C]	30	30	40	40	30	30	40	40
Optimized Process	Turbine inlet pressure [bar]	8.4	9.1	11.5	12.2	8.5	9.1	11.8	12.5
	Intermediate pressure level [bar]	2.34	2.34	2.40	2.40	2.34	2.34	2.40	2.40
	Water/steam flow rate [kg/s]	19.5	19.0	19.7	19.4	19.4	19.1	19.6	19.3
	Flow ratio to heat production [-]	0.21	0.21	0.21	0.21	0.21	0.21	0.21	0.21
OTSG core geometry	Diagonal tube pitch / tube OD	2.29	3	2.40	3	2.54	3.1	2.54	3
	Fin height [mm]	5.5	6.3	6.2	6.8	8.1	7.2	7.2	7.1
	Fin pitch [mm]	5.6	4.4	5.2	4.6	6.4	4.0	5.3	4.0
	Number of tube rows [-]	26	34	26	34	36	40	38	42
	Tube length [m]	4.0	3.7	4.5	3.8	4.4	4.7	4.2	4.1

Generally, thicknesses of the plates in a specific casing for a OTSG will be depending on the design of the critical parts as flanges, stiffeners, and their specific location on the plates. Most important is the arrangement of stiffener; stiffeners that connect continuously along the structure will have a stiffening effect and will cause stress concentration that will result in plastic strains and damage after only a few cycles (low cycle fatigue). The evaluated cases did not assess the effect of weaker stiffeners in combination with thinner casing plates, which could in turn reduce the higher plastic strains seen in cases with thinner plates. This and disconnected stiffeners are probably best for structures with low plate thickness. The recommendation that can be done from this assessment is to vary the stiffness of beam in accordance to plate thickness, and check for several ways to arrange the beams that allow the whole structure to better accommodate thermal expansion during operational cycles. The amount of plastic strains differ greatly for the different plate thicknesses and beam arrangements, see Fig. 14. That makes a general conclusion difficult to draw. The standard ISO 21905:2020 has some recommendations for design with regards to both hot and cold casing that should be followed to maximize lifetime. In the end, accurate design of an industrial case, with the right balance of stiffness in the stiffening beams and plates would lead to the lightest structure fitted for the purpose.

3.4. Water purification system: opportunities and challenges for weight reduction

3.4.1. Reduction of leaks

A typical offshore water purification system can weigh up to 110 tonnes total. Of this 41 tonnes is equipment and 75 tonnes are water sitting in the deaerator and make-up water tanks. Part of the reason for the high weight is the need to produce make-up water which in some extreme cases in earlier systems were found to be at the rate of 21 tonnes/day. The most effective ways to reduce weight of the water treatment system is to remove leaks and therefore reduce the need for make-up water and oversized treatment technologies to purify make-up water.

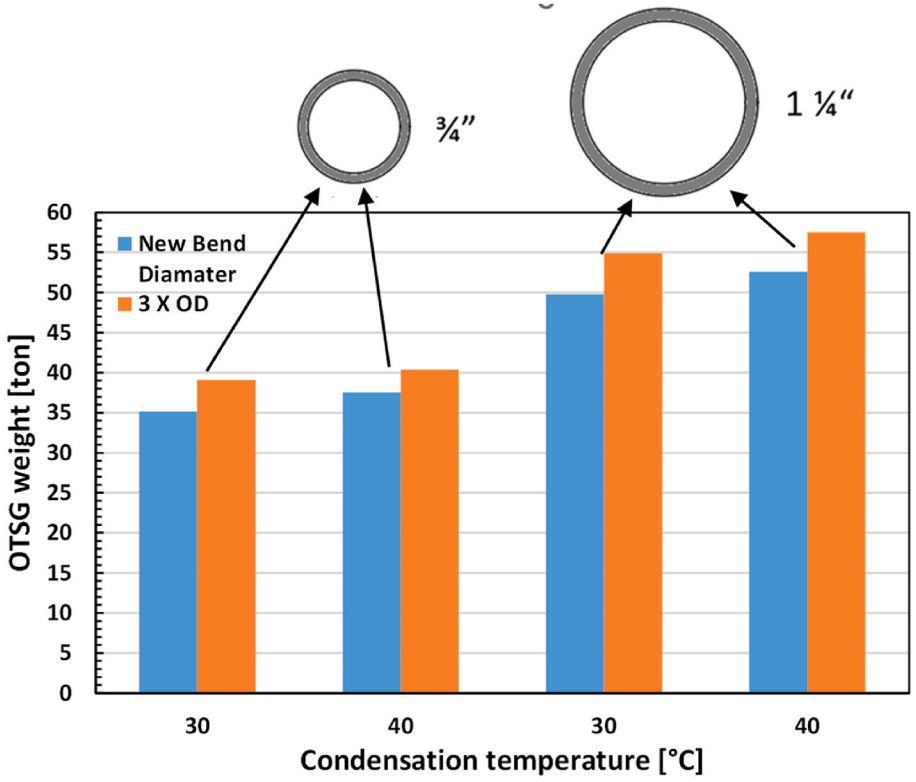

Fig. 10. Total weight of single OTSG for designs using previous bend limit (diagonal tube pitch 3 times the tube diameter 3 *x* OD) compared to the results with new bend diameter (present results). All cases have the same heat and power production. The first set on the left (30 °C - 40 °C) are related to the small tube diameter ¾" and the second set on the right (30ºC-40 °C) is related to greater tube diameter 1 ¼" tubes.

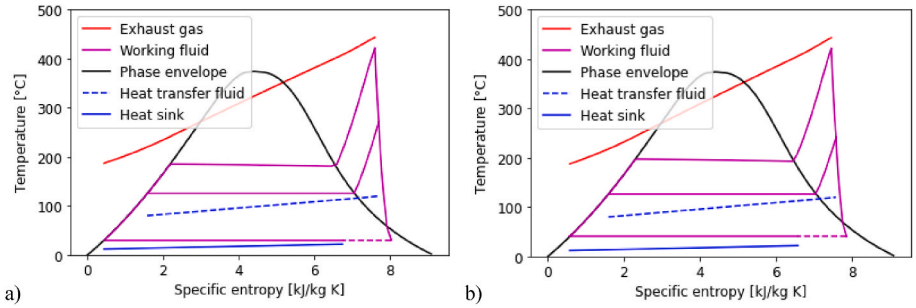

Fig. 11. T-s diagrams of the optimized bottoming cycle processes using the ¾” OTSG tubes. Condensation temperature 30 °C (a) and 40 °C (b).

3.4.1.1. Steam turbine. A key source of leaks is the steam turbine which has different stages and leaks occur between the different stages. Steam will try to escape out or atmospheric air will sneak in turbine gaps. For most onshore systems the evaporated water is recovered to prevent losses but that may not occur offshore due to increased complexity and weight of such systems. However, this leak may be a big contributor to the large size of the water purification beds and an optimization should be performed between acceptable turbine leak rate vs. size of turbine and size of water purifier. Steam will try to exit the turbine in the high-pressure zone. In the low-pressure zone the seal has to always be maintained as air can flow in. Steam traps are used to reduce the leakage.

3.4.1.2. Deaerator. Some steam is used to deaerate incoming boiler feed water. Steam strips the dissolved gas from the feedwater and exits via the vent valve. The vent line usually includes a valve and just enough steam is allowed to escape with the vented gases hence a plume of steam can be visible here. This loss is comparable to other steam losses throughout the steam/condensate system from leaking seals and valves that can be significant [42]. A deaerator is used with drum systems but may not be necessary in an OTSG system.

3.4.1.3. Condenser. From experience in the power industry, it is well known that the condenser that cools condensate by use of seawater is a source of leaks in the system. The most critical issue with these leaks is that seawater can enter the condensate stream and cause corrosion in the heat exchanger if it is not removed properly. It is therefore recommended to use a Na sensor following the condenser to rapidly detect potential leaks.

3.4.1.4. Operating pressure. Often systems are run at operating pressures that are too close to the safety pressure of valves to optimize performance. This often can set off leaks in the valves. A recommendation to minimize leaks is therefore to keep operating pressure 1–2 bars below safety pressure.

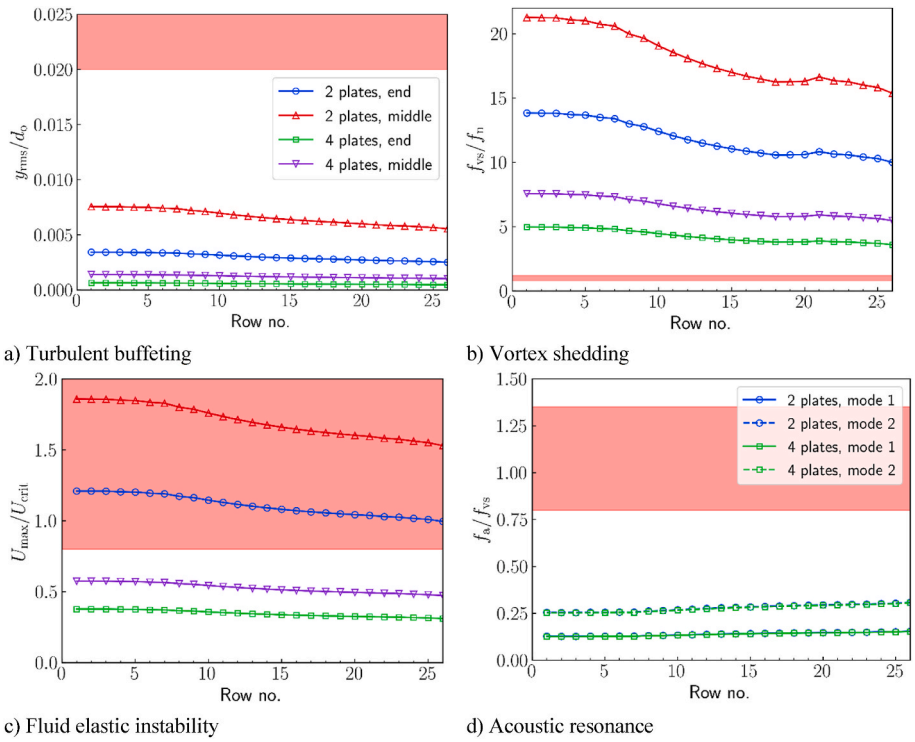

Fig. 12. Vibration analysis of the tube bundle in the case of ¾" OTSG tubes and condensation temperature 30 °C. (Row number 1 is the closest to the exhaust inlet, and red zone means the design criteria are not satisfied.)

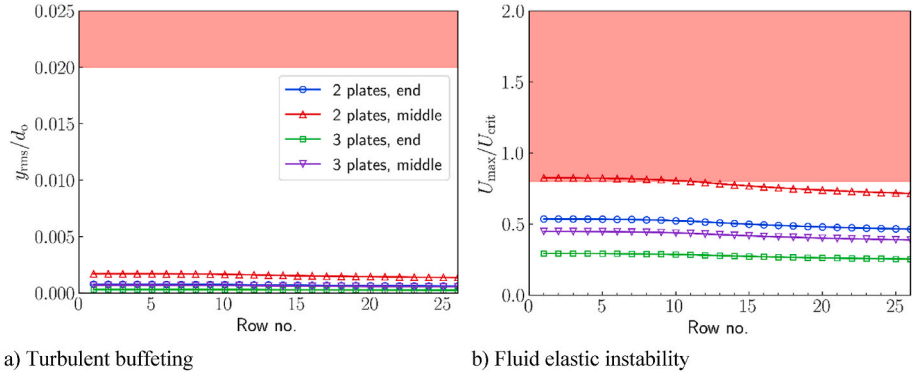

Fig. 13. Vibration analysis of the tube bundle in the case of 1¼" OTSG tubes and condensation temperature 30 °C. (Row number 1 is the closest to the exhaust inlet, and red zone means the design criteria are not satisfied).

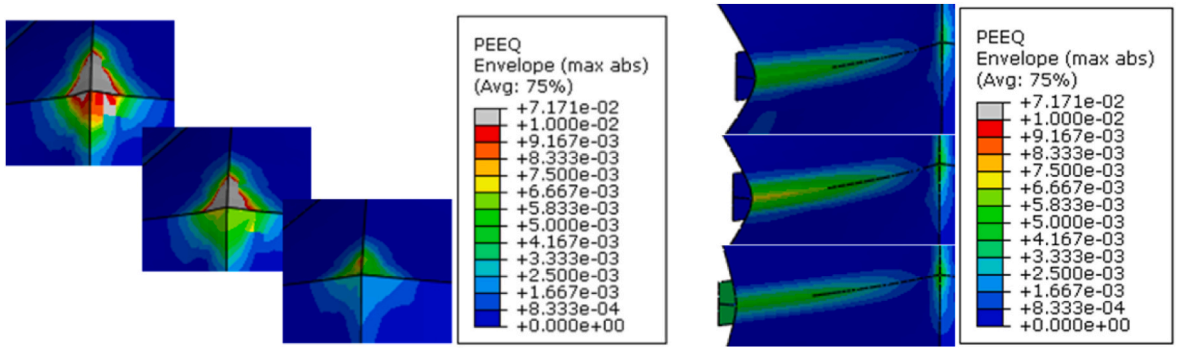

Fig. 14. Detail view for 3 different plate thickness (6, 8 and 12 mm from left, top) showing equivalent plastic strains after 2 cycles.

3.4.2. Technology switch to EDI

It was found in this study that switching water purification technology from ion exchange to electro-deionization would give a weight reduction as one can eliminate chemical tanks for regeneration. The disadvantages of switching to EDI would be an increased rate of water loss as EDI results in a 5–10% loss of water in the reject stream vs only 3% for ion exchange. The other issue is whether EDI would be reliable enough to work as a polishing technique in the water treatment system which could in case of leaks or influx of impurities become contaminated. It could be well suited for make-up water production from seawater following evaporation or reverse osmosis (RO) of seawater as the pretreated water then is of a consistent quality. Further research is needed on the best technology for condensate treatment.

It is possible to reduce the weight of the water treatment system by switching tank materials from steel to glass fibre reinforced polymer. By switching to plastics, and eliminating the chemical treatment system by switching to EDI and switching the framework for the installation of the water treatment system from steel to Aluminium significant weight reduction can be achieved. However, the greatest potential for weight reduction was in removing leaks.

4. Conclusions

In this work we have proposed and designed an efficient system for generating heat and power at an FPSO. This system consists of two gas turbines and a steam bottoming cycle. Focus was to minimize the weight by optimizing the thermodynamic design of the bottoming cycle and the geometric configuration of the OTSG. A novelty of this work is the proposal of a more compact and lightweight OTSG by using smaller bend diameter than current design practice. We have also demonstrated the importance of selecting small tubes for reducing the OTSG weight.

Vibration analysis is conducted, that supports the evaluation of flow induced vibrations, to find the required number of support plates. The numerical simulations in this work support the standard recommendations of using 35 times tube OD as upper limit for the unsupported tube length, which could be a reasonable criterion for an initial design at conceptual design phase.

Casing design is an important part of an OTSG design. Thermal expansion of material creates stresses on components at connections with other stresses, where the deformations are constrained. Deformations above elastic limit of the material cause non-reversible plastic deformations and damage the material. During their lifetime, heat exchangers are subject to many cycles of start and stop, heat up and cooldown. It has been investigated how plate thickness impacts the development of thermal stresses on a casing. What was observed here was that design, mostly on beam arrangement, location, stiffness of beams has a major impact on thermal stresses and can be optimized to different plate thicknesses in order to avoid fatigue damage.

Reducing leaks as much as possible is the key to reduce the weight of the water treatment system. Focus should be on potential deaerator, steam turbine and condenser. It is recommended to add Na sensors after condenser, as well as investigating the use of EDI for make-up water production from seawater following evaporation or RO. Research is still needed on best technology selection for condensate treatment.

Credit author statement

Rubén M. Montañés: Conceptualization, Methodology, Writing-Original Draft, Review & Editing, Investigation, Visualization, Project administration; Brede AL Hagen: Conceptualization, Methodology, Writing-Original Draft, Review & Editing, Software, Investigation, Formal Analysis, Data curation, Visualization; Han Deng: Conceptualization, Methodology, Writing-Original Draft, Review & Editing, Software, Investigation, Formal Analysis, Data curation, Visualization; Geir Skaugen: Conceptualization, Methodology, Writing-Review & Editing, Software, Investigation, Formal Analysis, Project administration; Nicolas Morin: Methodology, Writing-Original Draft, Review & Editing, Software, Formal Analysis, Investigation, Data curation; Marius Andersen: Methodology, Writing-Review & Editing, Investigation, Project administration; Marit J. Mazzetti: Conceptualization, Methodology, Writing-Original Draft, Investigation, Project administration.

Declaration of competing interest

The authors declare that they have no known competing financial interests or personal relationships that could have appeared to influence the work reported in this paper.

Data availability

The data that has been used is confidential.

Acknowledgements

The authors would like to acknowledge Conocophillips Scandinavia AS, Equinor Energy AS, NTNU, SINTEF, and the Research Council of Norway, strategic Norwegian research program PETROMAKS2 (#280713), for their support.

References

[1] Nord LO, Bolland O. Design and off-design simulations of combined cycles for offshore oil and gas installations. Appl Therm Eng 2013;54:85–91. https://doi.org/10.1016/j.applthermaleng.2013.01.022.
[2] Mazzetti MJ, Hagen B, Skaugen G, Lindqvist K, Lundberg S, Kristensen OA. Achieving 50% weight reduction of offshore steam bottoming cycles. Energy 2021. Vol 230. 120634.
[3] Deng H, Skaugen G, Næss E, Zhang M, Øiseth OA. A novel methodology for design optimization of heat recovery steam generators with flow-induced vibration analysis. Energy 2021;226:120325. https://doi.org/10.1016/j.energy.2021.120325.
[4] Barbosa YM, da Silva JAM, De O, Junior S, Torres EA. Deep seawater as efficiency improver for cogeneration plants of petroleum production units. Energy 2019;177:29–43.
[5] Carranza Y, Oliveira S. Assessment of the exergy performance of a floating, production, storage and offloading (FPSO) unit: influence of three operational modes. In: 28TH int. Conf. Effic. COST, optim. Simul. Environ. IMPACT ENERGY syst.; 2015. Pau, France.
[6] da Silva JAM, de Oliveira Junior S. Unit exergy cost and CO2emissions of offshore petroleum production. Energy 2018;147:757–66.
[7] Allahyarzadeh-Bidgoli A, Salviano LO, Dezan DJ, de Oliveira Junior S, Yanagihara JI. Energy optimization of an FPSO operating in the Brazilian Pre-salt region. Energy 2018;164:390–9. https://doi.org/10.1016/j.energy.2018.08.203.
[8] Kehlhofer F, Hannemann R, Stirnimann F, Bert R. Combined-cycle gas & steam turbine power plants. third ed. 2009.
[9] Gülen Can S, Kim K. Gas turbine combined cycle dynamic simulation: a physics based simple approach. ASME J Eng Gas Turbines Power 2014;136:011601. https://doi.org/10.1115/1.4025318.
[10] Beiron J, Montañés RM, Normann F, Johnsson F. Combined heat and power operational modes for increased product flexibility in a waste incineration plant. Energy 2020;202:117696. https://doi.org/10.1016/j.energy.2020.117696.
[11] Montañés RM, GarÐarsdóttir SÓ, Normann F, Johnsson F, Nord LO. Demonstrating load-change transient performance of a commercial-scale natural gas combined cycle power plant with post-combustion CO2 capture. Int J Greenh Gas Control 2017;63. https://doi.org/10.1016/j.ijggc.2017.05.011.
[12] Riboldi L, Nord LO. Lifetime assessment of combined cycles for cogeneration of power and heat in offshore oil and gas installations. Energies 2017;10:744. https://doi.org/10.3390/en10060744.
[13] Nguyen T-V, Tock L, Breuhaus P, Maréchal F, Elmegaard B. Oil and gas platforms with steam bottoming cycles: system integration and thermoenvironomic evaluation. Appl Energy 2014;131:222–37. https://doi.org/10.1016/J.APENERGY.2014.06.034.
[14] Montañés RM, Skaugen G, Hagen B, Rohde D. Compact steam bottoming cycles: minimum weight design optimization and transient response of once-through steam generators. Front Energy Res 2021;9:261.
[15] Nord LO, Martelli E, Bolland O. Weight and power optimization of steam bottoming cycle for offshore oil and gas installations. Energy 2014;76:891–8. https://doi.org/10.1016/J.ENERGY.2014.08.090.
[16] Brady MF. Design aspects of once through systems for heat recovery steam generators for base load and cyclic operation. Mater A T High Temp 2001;18:223–9. https://doi.org/10.1179/mht.2001.024.
[17] Nguyen T-V, Tock L, Breuhaus P, Maréchal F, Elmegaard B. Thermo-economic modelling and process integration of CO2-mitigation options on oil and gas

platforms. Chem Eng Trans 2014;39:1081–6. https://doi.org/10.3303/CET1439181.
[18] Zhao GY, Liu YL, Dong CS, Yang H, Fan XG. Analysis of wrinkling limit of rotary-draw bending process for thin-walled rectangular tube. J Mater Process Technol 2010;210:1224–31. https://doi.org/10.1016/j.jmatprotec.2010.03.009.
[19] Khodayari G. Bending limit curve for rotary draw bending of tubular components in automotive hydroforming applications. SAE Int J Mater Manuf 2009;1:841–8.
[20] Ghiotti A, Simonetto E, Bruschi S. Insights on tube rotary draw bending with superimposed localized thermal field. CIRP J Manuf Sci Technol 2021;33:30–41. https://doi.org/10.1016/j.cirpj.2021.02.012.
[21] Yang H, Li H, Ma J, Li G, Huang D. Breaking bending limit of difficult-to-form titanium tubes by differential heating-based reconstruction of neutral layer shifting. Int J Mach Tool Manufact 2021;166:103742. https://doi.org/10.1016/j.ijmachtools.2021.103742.
[22] Nord LO, Montañés RM. Compact steam bottoming cycles: model validation with plant data and evaluation of control strategies for fast load changes. Appl Therm Eng 2018;142. https://doi.org/10.1016/j.applthermaleng.2018.07.012.
[23] Rúa J, Bui M, Nord LO, Mac Dowell N. Does CCS reduce power generation flexibility? A dynamic study of combined cycles with post-combustion CO2 capture. Int J Greenh Gas Control 2020;95:102984. https://doi.org/10.1016/j.ijggc.2020.102984.
[24] Zotică C, Montañés RM, Reyes-Lúa A, Skogestad S. Control of steam bottoming cycles using nonlinear input and output transformations for feedforward disturbance rejection. IFAC-PapersOnLine 2022;55:969–74. https://doi.org/10.1016/j.ifacol.2022.07.570.
[25] Viswanathan R, Stringer J. Failure mechanisms of high temperature components in power plants. J Eng Mater Technol 2000;122:246–55. https://doi.org/10.1115/1.482794.
[26] Païdoussis MP. Real-life experiences with flow-induced vibration. J Fluid Struct 2006. https://doi.org/10.1016/j.jfluidstructs.2006.04.002.
[27] Stoppato A, Mirandola A, Meneghetti G, Lo Casto E. On the operation strategy of steam power plants working at variable load: technical and economic issues. Energy 2012;37:228–36. https://doi.org/10.1016/J.ENERGY.2011.11.042.
[28] Choi W HYUNJ. A life assessment for steam turbine casing using inelastic analysis. Mod Phys Lett B 2008;22:1141–6. https://doi.org/10.1142/S0217984908015978.
[29] Dubey A, Relan R, Lohse U, Szwedowicz J. A Nonlinear Dynamic Reduced-Order Model for a Large Gas Turbine Outer Casing Low Cycle Fatigue Prediction 2021. https://doi.org/10.1115/GTINDIA2021-76056.
[30] Zhang M, Øiseth O, Petersen ØW, Wu T. Experimental investigation on flow-induced vibrations of a circular cylinder with radial and longitudinal fins. J Wind Eng Ind Aerod 2022;223:104948. https://doi.org/10.1016/j.jweia.2022.104948.
[31] Zhang M, Øiseth O. Fluidelastic instability of tube arrays in nonuniform flow: effect of multimode coupling. J Fluid Struct 2022;110:103545. https://doi.org/10.1016/j.jfluidstructs.2022.103545.
[32] Zhang M, Wang X, Øiseth O. Numerical simulation and modeling convention of unsteady fluidelastic forces of tube arrays. J Pressure Vessel Technol 2021:144. https://doi.org/10.1115/1.4052694.
[33] Mazzetti M, Skaugen G. Electro deionization for treatment of condensate of steam bottoming cycles. J Clean Prod 2023.
[34] Hagen BAL. Gradient-based design optimization and off-design performance prediction of Rankine cycles and Radial Inflow Turbines. Norwegian University of Science and Technology; 2022.
[35] Raddum A. Transient performance of Siemens SGT-750 and SGT800 modeling and simulations of industrial gas turbines on island grids. Umeå Unviersity; 2020.
[36] Schittkowski K. {NLPQL}: a fortran subroutine solving constrained nonlinear programming problems. Ann Oper Res 1986;5:485–500.
[37] Wagner W, Pruß A. The IAPWS formulation 1995 for the thermodynamic properties of ordinary water substance for general and scientific use. J Phys Chem Ref Data 2002;31. https://doi.org/10.1063/1.1461829.
[38] Skaugen G, Walnum HT, Hagen BAL, Clos DP, Mazzetti MJ, Nekså P. Design and optimization of waste heat recovery unit using carbon dioxide as cooling fluid. Am. Soc. Mech. Eng. Power Div. POWER 2014;1. https://doi.org/10.1115/POWER2014-32165.
[39] Mentella A, Strano M, Gemignani R. A new method for feasibility study and determination of the loading curves in the rotary draw-bending process. Int J Material Form 2008;1:165–8. https://doi.org/10.1007/s12289-008-0017-0.
[40] Ku T-W, Cha J-H, Kim Y-B, Kwak O-G, Kim W-S, Kang B-S. A study on process parameters for cold U-bending of SUS304L heat transfer tube using rotary draw bending. J Mech Sci Technol 2013;27:3053–61. https://doi.org/10.1007/s12206-013-0825-0.
[41] Kang S-K, Kim Y-C, Kim K-H, Kwon D, Kim J-Y. Constitutive equations optimized for determining strengths of metallic alloys. Mech Mater 2014;73:51–7. https://doi.org/10.1016/j.mechmat.2014.01.010.
[42] Inveno Engineering LLC. Causes of Steam Leakage n.d. https://invenoeng.com/causes-of-steam-leakage/(accessed June 7, 2023).